Improved CaO-based materials for thermochemical energy storage in concentrated solar power applications

David Piqué Prat

david.pique@tecnico.ulisboa.pt

Instituto Superior Técnico, Universidade de Lisboa, Portugal, October 2022

K e y w o r d s

Thermal energy storage

Calcium looping

CaO-based materials

Sol-gel method

Sintering

Concentrated solar power

A B S T R A C T

CaL looping is considered a promising technology as it combines thermochemical energy storage (TCES) technology with concentrated solar power (CSP) plants to improve system efficiency. The objective of this thesis is to prepare different CaO-based materials by the sol-gel method with improved properties (higher porosity, stability and solar absorbance) for CaL. Furthermore, the effect of steam on the reactivity and stability of the materials throughout the CaL process will be studied. The CaL experiments were conducted in a fixed-bed unit over 10 calcination-carbonation cycles, with calcination and carbonation temperatures of 930 ºC and 800 ºC, respectively. The selected dopant materials were: Methocel™, SiC, MgO and CeO_2. TGA, XRD, SEM, and N_2 adsorption methods were used to examine mineralogical, textural, and morphological properties before and after the 10 cycles. A sorbent synthesised using the sol-gel method and composed by 100 % of CaO was used as a reference. In this work, the use of steam had no long-term benefit on sorbent reactivity, even with higher S_{BET} than the reference. Methocel™/CaO-based sorbents showed a low level of deactivation, a small reduction in S_{BET}, and a small increase in crystallite size, however its performance in CaL is lower than the reference. The SiC/CaO-based sorbents showed by far the worst results, with high deactivation levels. CeO_2/CaO-based sorbents obtained a slightly worse results than the reference. The best results were obtained by the MgO/CaO-based sorbents, more specifically with 10% of MgO, increasing the heat storage density (HSD) of commercial $CaCO_3$ by 121%.

1. I N T R O D U C T I O N

Currently, global electricity demand exceeds the capacity of renewable and nuclear energy sources, so gas and coal-fired power plants are responsible for closing the gap. According to the International Energy Agency (IEA), global electricity demand will increase by 30 % in 2030 compared to 2020 and by 80 % in 2050 [1]. EU Commission proposed in 2020, the 2030 Climate Target Plan which aims to reduce greenhouse gas emissions by at least 55 % by 2030 in Europe [2] and to be climate neutral (net-zero greenhouse gas emissions) by 2050. Given this reality, it is absolutely necessary to develop new sustainable technologies or improve the efficiency of existing ones.

Renewable energy sources have been increasing their presence considerably, but the energy transition cannot be definitive if the intermittent energy supply provided by renewables sources cannot be compensated. Concerning solar thermal systems, Thermal Energy Storage (TES) has become a promising solution for energy storage in combination with Concentrated Solar Power (CSP) plants. With the implementation of TES in CSP plants, heat can be stored during periods of high solar radiation (charging period) and released when radiation is low (discharge period). Thus, the limitations imposed by climatic conditions can be overcome. At the moment, there are 3 types of TES: sensible thermal energy storage (STES), latent thermal energy storage (LTES) and thermochemical energy storage (TCES). Their technology is based on the variation of sensible temperature, latent temperature (phase change) and chemical reactions, respectively. Among the three types of TES, TCES is recognized as having the highest potential for stable and efficient energy generation due to its inherent advantages: high heat storage density (HSD) (nearly 1000 kJ/dm^3), long term storage, smaller storage volume, and no heat loss [3].

TCES can be separated according to the type of reaction into reversible chemical reactions or sorption processes. The sorption process is based on the capture of a gas or vapour within a sorbent while reversible chemical reactions are characterised by a change in the molecular configuration of the involved compounds. In reversible chemical reactions, thermal energy is supplied during the endothermic reaction and released during the exothermic reaction. TCES consists

of three main phases [4]: charging, storage and discharging. The charging phase is an endothermic reaction as the thermal energy is used to dissociate the chemical reactant AB into the products A and B. After charging, the sensible heat contained in products A and B is recovered in a heat exchanger. These products are separated and stored at ambient temperature. Subsequently, the products are preheated to reaction temperature before the discharge phase begins. In the discharge phase, the products A and B are combined and re-form the reactant AB by an exothermic reaction.

The thermochemical material used in this thesis will be CaO_3 (CaO/CO_2 pair) because of its high storage energy storage density and high reaction temperature as well as its ability to react with the CO_2. The use of natural CaO-based materials as the CO_2 sorbent is a simple and cost-effective method for Calcium Looping (CaL) process [5]. The CaL process is composed of two reactions: calcination and a carbonation. The calcination (Eq 1) is an endothermic reaction where $CaCO_3$ is decomposed, the products CaO and CO_2 are formed, and the enthalpy variation of the reaction is positive. The carbonation (Eq 2) is an exothermic reaction where CaO and CO_2 are combined, $CaCO_3$ is formed again and the enthalpy variation of the reaction is negative.

$$CaCO_3(s) \rightarrow CaO(s) + CO_2(g) \qquad \Delta H_{900\,°C,1\,bar} = 165\frac{kJ}{mol} \qquad (1)$$

$$CaO(s) + CO_2(g) \rightarrow CaCO_3(s) \qquad \Delta H_{700\,°C,1\,bar} = -170\frac{kJ}{mol} \qquad (2)$$

The CaL process is based on the cyclic calcination-carbonation reaction of CaO-based materials, which was recognised as the most promising of the TCES systems presented for large scale. However, after evaluating various CaO-based materials, a rapid decrease in CO_2 capture was detected after each cycle due to the sintering of the sorbent, leading to a reduction in surface area and poor structural stability. Sintering is produced by high temperatures and the presence of contaminants in the reaction environment, as related to the fragile structure of unsupported CaO-based sorbents [6]. In response to this drawback, synthetic CaO-based sorbents were developed to prevent this decrease in reactivity [7].

2. EXPERIMENTAL SECTION

2.1 Sorbents and inerts supports

In order to prepare the unsupported CaO sorbents, calcium nitrate tetrahydrate ($Ca(NO_3)_2.4H_2O$) from Sifma-Aldrich (assay ≥ 99 %) and citric acid monohydrate ($C_6H_8O_7.H_2O$) from Panreac (assay of 99,5–102 %) were dissolved in distillate water, with a molar ratio of distillate water and citric acid to calcium nitrate of 120:1 and 1:1, respectively. On the other hand, to prepare the supported CaO sorbents, four different types of supports were used: Methocel™ F4M (a water-soluble hydroxypropyl methylcellulose polymer) from DOW, silicon carbide with 37 µm of size (also known as carborundum) from VWR-Prolabo, magnesium nitrate hexahydrate ($Mg(NO_3).6H_2O$) from Sigma-Aldrich (assay of 98–102%) and cerium nitrate hexahydrate ($Ce(NO_3).6H_2O$) from Sigma-Aldrich (assay ≥ 99%). Methocel™ was selected to increase the porosity of the sorbent and SiC was chosen because its dark colour can improve the absorption of solar radiation from the sorbent. MgO and CeO_2 were chosen for their high sintering temperature. In addition, CeO_2 enhances pore formation and has a high dispersion. Table 1 lists all the samples prepared for the 16 experiments carried out in this work.

All the solutions were stirred with magnetic bars in a silicone oil bath at 80 ºC for 6-8h, depending on how long it takes the gel to form and stop the rotation of the magnetic bar. The wet gel was then dried in an oven at 120 °C overnight. After drying, the sample was calcined in the muffle by ramping the temperature to 800 °C at a rate of 5 °C/min, followed by further 3 hours at 800 °C. In the case of CeO_2, the rate had to be reduced to 2.5 ºC/min because with a ramp of 5 °C/min the sample burst in the muffle, probably due to the high and rapid volume increase that causes an internal overpressure.

Table 1 – Summary of the mass composition of unsupported and supported CaO sorbents.

Sample ID	Support Material	CaO mass fraction (%)	Support mass fraction (%)
SG 1	n.a.	100	0
SG 2	Methocel™	90	10
SG 3	SiC	90	10
SG 4		80	20
SG 5		70	30
SG 6	MgO	90	10
SG 7		80	20
SG 8		70	30
SG 9	CeO_2	90	10
SG 10		80	20
SG 11		70	30
SG 12	MgO and CeO_2	80	10MgO/ 10CeO_2

n.a. – not applicable

2.2 Characterization methods

The mineralogical characterization of the fresh sorbents was obtained using X-ray powder diffraction (XRD). The Diffractometer used to carry out the study was the Bruker D8 Advance equipped with a 1D detector (SSD 160), a Cu Kα radiation (λ=0.15405 nm) and a Ni filter. It was operated at 40 kV and 30 mA collecting It collected data between 5 and 80° (2θ) with a step size of 0.03° and a step time of 0.5 s.

Textural properties of fresh and spent sorbents were obtained using the N_2 sorption technique. The autosorb IQ from Quantachrome Instruments evaluated nitrogen adsorption at a temperature of -196 °C (77 K) and required a previous degasification operation to prevent other gases or contaminants. The procedure that followed was carried out under vacuum and consisted of two steps: the first at 90 °C for 1 hour and the second at 350 °C for 5 hours. The software ASIQwin was used to collect and analyse the sorbent's specific area (S_{BET}) using the BET method; the pore size distribution using BJH desorption model; and the total pore volume (V_p) at a relative pressure (p/p_0) of 0.97 using the nitrogen isotherm. Morphological properties of fresh and spent sorbents were analysed via scanning electron microscopy (SEM) by the Phenom Pro G6 from Thermo Scientific.

Thermal properties of the fresh sorbents were obtained using thermogravimetric analysis (TGA) conducted in TG-DTA/DSC Setsys Evo 16 device. The wet sol gel samples (~10 mg) were heated at a constant rate of 10 °C.min^{-1} from room temperature until 900 °C, under air atmosphere, and the weight loss, the DTG and the heat flow was registered. A blank experiment was also conducted to correct the mass changes related with the gas density that is affected by the temperature. The software used for the data processing was Calisto.

2.3 Calcium looping for TCES setup

A fixed bed reactor was used to evaluate the reactivity and stability of the sorbents during the calcination-carbonation cycles of the CaL process at laboratory scale. This unit is composed of two elements: an oven and a quartz reactor. The oven has 10 cm of diameter, 30 cm high and is internally coated with ceramic to promote heat transfer to the quartz reactor. The quartz reactor is resistant to high temperatures and measures 14 cm of high and 5 cm of internal diameter. To ensure that the calcination and carbonation temperature is reached during the cycles, the Eurotherm® 2000 controller system is used. This controller is connected to a type K thermocouple which is inserted into a thermowell near the sorbent in order to assess the reactor and sample temperature. The gases fed into the reactor were monitored using flowmeters from Alicat Scientific (MC Series) for air flow and Brooks (5850E Series) for CO_2. To measure the amount of CO_2 in the outlet gas, the exhaust gas flow was connected to a CO_2 gas concentration analyzer. The Guardian NG with a CO_2 concentration range of 0-100 % and 2% full-scale accuracy was used.

In order to generate steam, the dry gas stream (air and CO_2) was passed through a water bubbler system that includes a saturator (gas washing bottle) that was filled with distilled water and submerged in a thermostatic bath. When leaving the quartz reactor, the steam passes through a vapour separator which is located inside a container with ice. As the gas flow is cooled, the vapour is condensed and the water is accumulated in

the vapour separator, thus eliminating the vapour contained in the gas flow. A molar fraction of 5 %, 9 % and 17 % was considered for SG1 and a 9% for SG12.

The data acquisition was performed using the LABVIEW software. Through its software specially designed to track the reactor temperature and the CO_2 flow rate in the outlet, the evolution of the cycles over the time can be visualised, thus facilitating the correct shift of temperatures.

For each experiment was used ca.1 gram that was uniformly distributed in the quartz reactor. Each test consisted of 10 calcination-carbonation cycles where calcination is carried out for 10 minutes and carbonation until the CO_2 flux at the outlet is stabilised at 50%. The operating atmosphere is balanced by a CO_2 flow and an air flow, both at 500 ml/min. Regarding operating conditions, the most promising temperatures for TCES have been proposed from the Teixeira *et al.* [8] study: 800 ºC for carbonation and 930 ºC for calcination.

3. RESULTS AND DISCUSSION

3.1 Characterization of fresh sorbents

In the fresh materials pre-calcinated at 800 ºC, the mineralogical properties were as expected. The characteristic peaks of CaO are observed in the XRD patterns of all sorbents. In some sorbents $CaCO_3$ appears due to the facility of CaO to react with CO_2. $Ca(OH)_2$ has also appeared with lower intensity peaks, which can be explained by the high rate hydration caused by atmospheric moisture exposure [9]. The peaks of the dopant materials (SiC, MgO and CeO_2) were detected in their corresponding samples.

The N_2 soprtion isotherms of all sorbent isotherms have a similar shape that is a combination of the Type II and IV isotherms, which are typical profiles of non- porous material or indicates the presence of macropores (Type II), but the hysteresis means that some mesopores are also present (Type IV). They display a Type H2(b) and H3 hysteresis which is common in more complex structures with important network effects, which results in pore-blocking in wider pore necks (H2(b) hysteresis loop) and of macropores not completely filled with pore condensate (H3 hysteresis loop).

Regarding thermal properties, all sorbents show a lower mass loss at 900 °C and a higher $CaCO_3$ decomposition temperature than SG1. As a result, the use of dopant materials had no positive effect, as a higher energy consumption is required to decompose $CaCO_3$.

Table 2 contains the specific surface area and the total pore volume values obtained through nitrogen adsorption. The variation with respect to the SG1 is also provided. In general, the values do not have a very significant variation.

Table 2 – Specific surface area (S_{BET}) and total pore volume (V_p) of synthetized sol-gel materials after calcination at 800 °C: SG1 (100 CaO), SG2 (90CaO/10Methocel™), SG3 (90CaO/10SiC), SG5 (70CaO/30SiC), SG6 (90CaO/10MgO), SG8 (70CaO/30MgO), SG9 (90CaO/10CeO_2), SG11 (70CaO/30CeO_2) and SG12 (80CaO/10MgO/10CeO_2).

Sorbents	Inert support	S_{BET} (m^2/g)	S_{BET} variation respect SG1 (%)
SG1	n.a.	33,2	-
SG2	Methocel™	26,1	-21,3
SG3	SiC	30,9	-6,8
SG5		31,8	-4,1
SG6	MgO	33,9	2,3
SG8		25,6	-22,9
SG9	CeO_2	23,1	-30,3
SG11		36,4	9,9
SG12	MgO/CeO_2	29,3	-11,8

n.a. – not applicable

From the images obtained by SEM analysis (Figure 1), the sorbents with the best morphological properties (porous, dispersed and ramified structure) are SG1, SG2, SG6 and SG12 without steam.

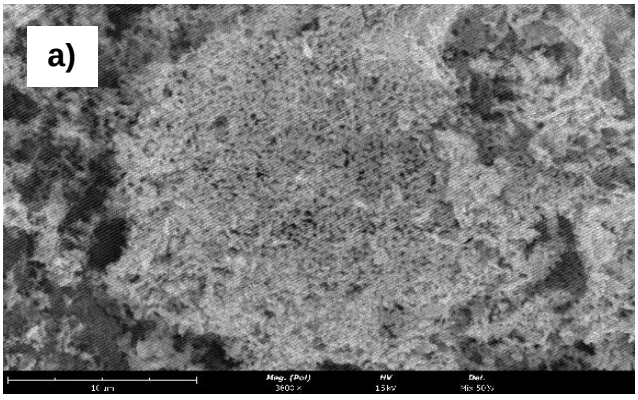

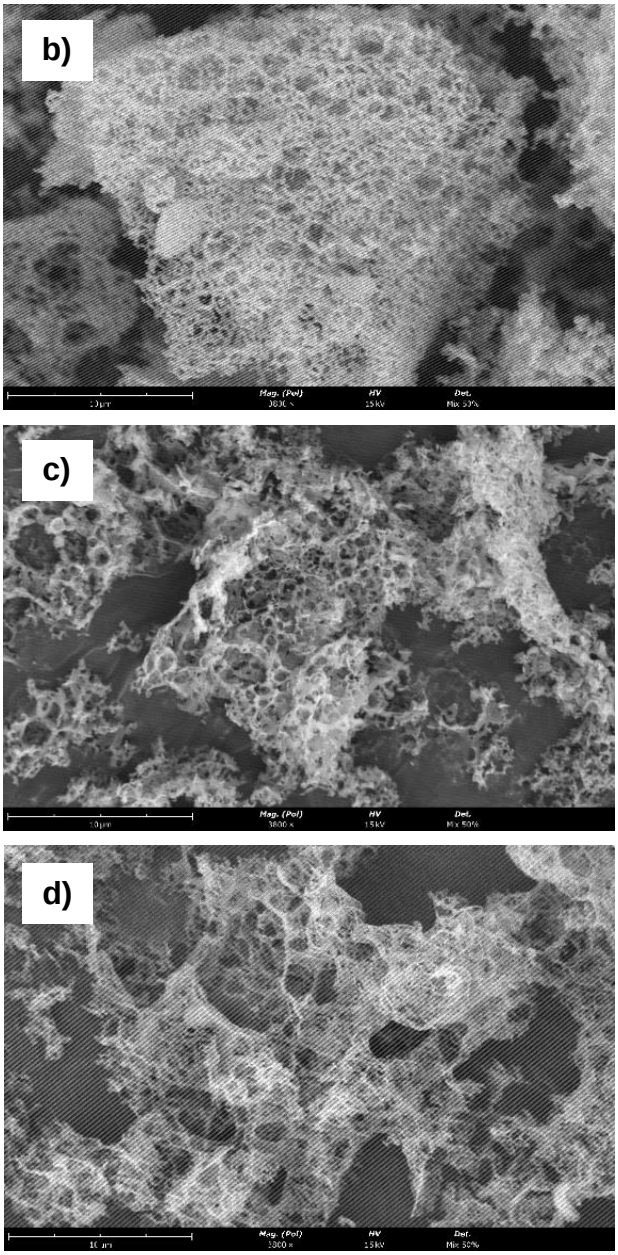

Figure 1 – SEM images of synthetized sol-gel materials after calcination at 80 °C: a)SG1-100 CaO; b)SG2-90CaO/10Methocel™; c) SG6 - 90CaO/10MgO and d) SG12-80CaO/10MgO/10CeO_2. All images have a scale of 10 µm and magnification of x3800.

3.2 CaL performance and characterization of CaO-based sorbents using steam injection

Looking at the Figure 2, it's clear that the experiment with the highest injected steam fraction has the worst performance. Perhaps the effect of the steam in small fractions can improve the sorbent performance during the first cycles, but in the long term it seems that its effect is not significant. A possible solution to this problem would be to reduce the calcination temperature, as steam has a higher thermal conductivity than air so it can transfer heat faster, thus allowing to reduce the temperature of the calcination reaction to delay the sorbent sintering.

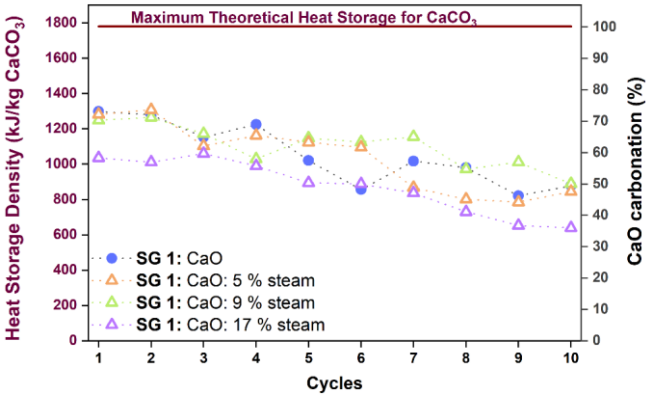

Figure 2 – Heat storage density (kJ/kg $CaCO_3$) and CaO (carbonation (%) of SG1 (100CaO) without steam and with 5 %, 9 % and 17 % of steam over 10 calcination-carbonation cycles carried out on a fixed bed unit.

After 10 cycles, S_{BET} and V_p have decreased in all samples. Also, the more steam is injected, the more S_{BET} and V_p increase. This seems to be against the previous results since the sample with the highest fraction of steam is the one with the worst performance. However, this S_{BET} is given by the increase of the pore volume in the range of 3-10 nm, which have a negative effect on CaL, as it contributes to pore plugging.

For the 5 %, 9 % and 17 % steam injected, the value of this increase is 74,35 %, 69,93 %, and 91,41 %, respectively, suggesting that the steam injection causes the crystallite size to increase. In the SEM images, in the cases where steam has been injected, the effects of sintering are magnified since large agglomerations of crystallites are formed and much porosity is lost.

3.3 CaL performance and characterization of supported CaO-based sorbents

The performance of the Methocel™/CaO-based sorbent over the cycles is shown in Figure 3. It is observed that the HSD is lower than SG1 over all the cycles. On the other hand, as a positive point, SG2 has a high stability throughout the cycles since its deactivation is 23 % while SG1 deactivation is 32 %.

The S_{BET} reduction of SG2 after 10 cycles is much smaller than SG1. This reduction has a value of 17.3 % and 71.2 %, respectively. In contrast to typical sintering

and pore size change models, the sorbent's pore size has been observed to decrease towards the 20-30 nm range, so a better performance should be expected. This phenomenon can be explained according to the pore-skeleton model by Manovic *et al.*[10], which explains the existence of a hard internal skeleton formed by the thermal decomposition of the organic components during calcination. Over the cycles, the skeleton becomes softer, modifying the morphology of the sorbent and enhancing the formation of small pores. From the SEM images, the SG2 after the cycles has a less ramified structure with some areas with particle agglomeration due to sintering.

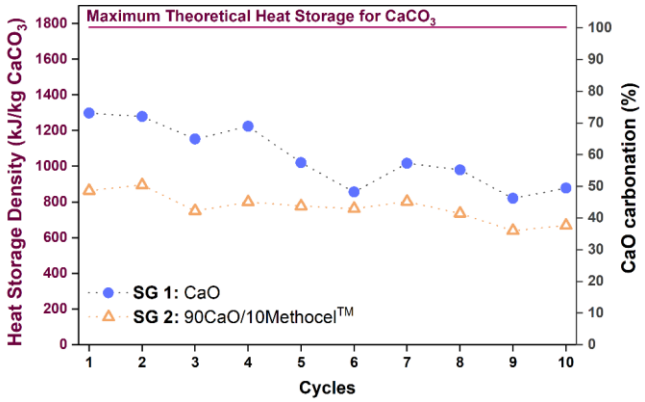

Figure 3 – Heat storage density (kJ/kg $CaCO_3$) and CaO (carbonation (%) of SG1 (100CaO) and SG2 (90CaO/10methocel™), over 10 calcination-carbonation cycles carried out on a fixed bed unit.

The performance of SiC/CaO-based sorbents, showed in Figure 4, are the worst results by far, with deactivation levels above 73% in all three samples. The S_{BET} loss is so large that it exceeds the LoQ (2 m^2/g) of the equipment, the mesopores observed in the fresh

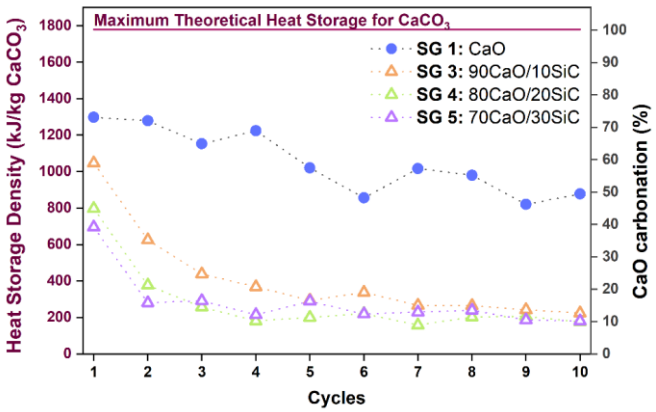

Figure 4 – Heat storage density (kJ/kg $CaCO_3$) and CaO carbonation (%) of SG3 (90CaO/10SiC), SG4 (80CaO/20SiC), and SG5 (70CaO/30SiC), over 10 calcination-carbonation cycles carried out on a fixed bed unit (SG1 is illustrated for comparison).

materials disappear after cycling and the increase in crystallite size is the largest of all samples (around 200%). Being a non-porous material with a high thermal conductivity [11] that promotes sintering, its implementation in the CaL for TCES is not recommended.

The performances obtained by the MgO/CaO-based sorbents are represented in Figure 5. The sample with a 10 % MgO fraction (SG6) has obtained the best profile with an HSD of 1088 kJ/kg $CaCO_3$ in the 10th cycle. The deactivations for SG6, SG7 and SG8 are 31 %, 35 % and 49 % respectively. SG6 has a S_{BET} reduction of 36.2 %, much lower than SG8 and SG1, with reductions of 51.3 % and 71.4 % respectively. Considering these variations during CaL, it seems that MgO provides a higher S_{BET} stability. In SG6 and SG8, the pore volume of the larger mesopores (30-100 nm) was reduced due to sintering. Regarding the crystallite size of the samples, no significant differences are observed between the samples.

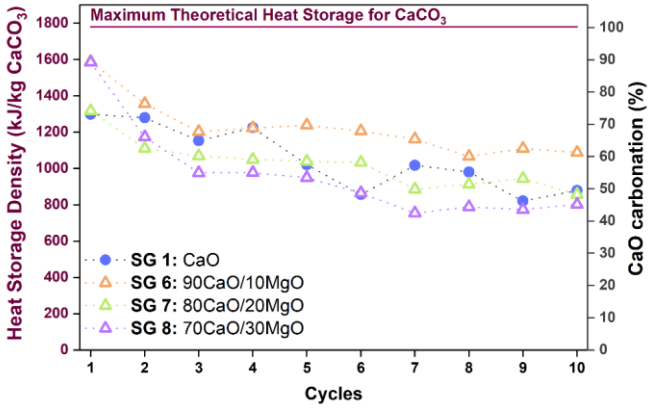

Figure 5 – Heat storage density (kJ/kg $CaCO_3$) and CaO carbonation (%) of SG6 (90CaO/10MgO), SG7 (80CaO/20MgO), and SG8 (70CaO/30MgO), over 10 calcination-carbonation cycles carried out on a fixed bed unit (SG1 is illustrated for comparison).

The SG6 SEM images reveal a dispersed and quite ramified structure, while the SG8 structure is more dense and compact, with a total loss of ramification and very low surface porosity.

Figure 6 represents the HSD profiles of the CeO_2/CaO-based sorbents. All the profiles are very similar, but none of the CeO_2/CaO-based samples perform better than SG1. They all have similar deactivation values: 51 % for SG9, 50 % for SG10, and 52 % for SG11. S_{BET}

reductions in SG9 are 49.8 % and 23.1 %, respectively, both lower than the 71.4 % reduction in SG1. However, the effects of sintering are clearly visible when the size pore distribution was examined for both samples. The amount of mesopores and small macropores decreases after the cycles. As a result, the advantage gained by the high S_{BET} of the CeO_2/CaO-based sorbents is mitigated by the reduction of 10-100 nm pores size, which are considered the ideal pore size for CaL, justifying the sorbents low performance after the first's cycles.

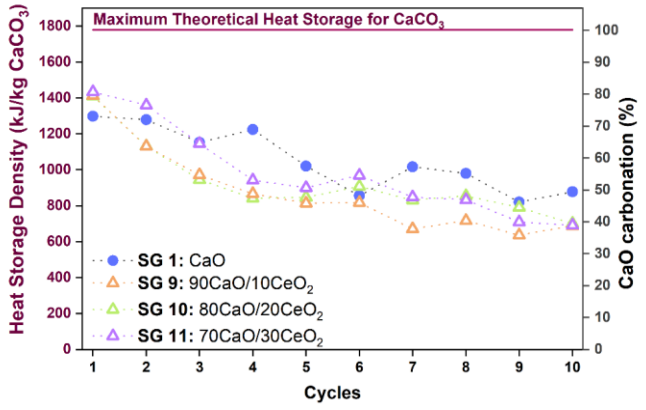

Figure 6 – Heat storage density (kJ/kg $CaCO_3$) and CaO carbonation (%) of SG9 (90CaO/10CeO_2), SG10 (80CaO/20 CeO_2), and SG11 (70CaO/30 CeO_2), over 10 calcination-carbonation cycles carried out on a fixed bed unit (SG1 is illustrated for comparison).

There is little difference in crystallite size between the samples: 59.1 % in SG9, 48.0 % in SG10, and 51.0 % in SG11. The structure of SG9 is dense and smooth, with more sharp shapes and large surface pores. The sample in SG11 appears more dispersed and less compact than in SG9. The surface of SG9 is smooth and has large pores, whereas the surface of SG11 is granular and has smaller and irregular pores. Due to its low performance and high production cost compared to MgO [12], the use of CeO_2 as a dopant in CaL under these operating conditions is questionable.

The HSD profiles of the MgO/CeO_2/CaO-based sorbents are shown in Figure 7. As shown in the graph, SG12 without steam injection has a better performance than SG1 and SG12 with steam. Both samples had a high reactivity in the first cycles, but it decreased as the cycles progressed. The decrement was accentuated in the case of steam injection, finishing with an HSD value of 741 kJ/kg $CaCO_3$ in the 10th cycle and a 52 % deactivation. On the other hand, SG12 without steam has a deactivation of 37 % and an ending HSD value of 997 kJ/kg $CaCO_3$, the second best of all samples.

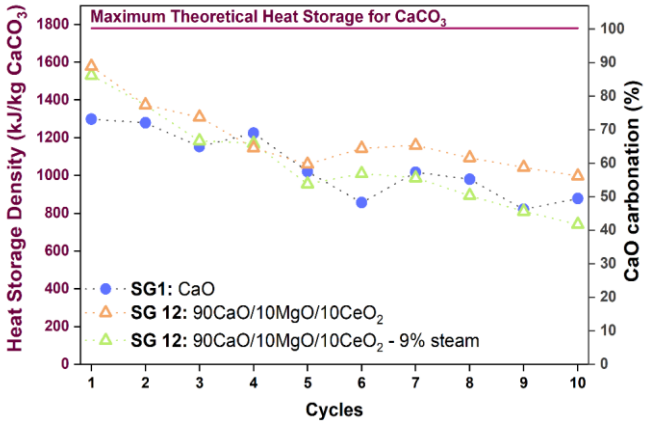

Figure 7 – Heat storage density (kJ/kg $CaCO_3$) and CaO carbonation (%) of SG12 (80CaO/10MgO/10CeO_2) without steam and with 9 % of steam over 10 calcination-carbonation cycles carried out on a fixed bed unit (SG1 is illustrated for comparison).

The S_{BET} in both cases is similar to that of SG1, with a reduction of 71.0 % without steam and 63.8 % with steam. The crystallite increase in SG12 without steam is 113.2 %, while it is 190.6 % in SG12 with steam, which is significantly higher than SG1. This confirms that the higher thermal conductivity of steam (~120 $mWm^{-1}K^{-1}$ at 900 ºC) in comparison with air/CO_2 (~76 and ~74 $mWm^{-1}K^{-1}$ at 900 ºC and 775 ºC [13], respectively) impacts negatively on the sorbents crystallite size.

Looking at the SEM images,he sample without steam injection has a branched structure but shows signs of sintering as the particles are rounded due to the melting between them. The sample with steam injection, on the other hand, has lower surface porosity, compact and dense zones, and a granular surface.

3.4 Sol-gel efficience for TCES compared to natural sorbents

Considering the SG1 as reference, only three of the 15 samples tested improved the reactivity profile during CaL: SG1-9 % steam, SG6 and SG12. The reactivity of the sorbent depends on multiple factors, but the higher the S_{BET} the better the performance during carbonation [14]. Regardless of SiC/CaO-based sorbents, the use of

inert dopants has managed to maintain a higher S_{BET} than SG1 after 10 cycles.

Finally, the results obtained with this study have been compared with the study of Teixeira *et al.* [8] since in both cases the same operating conditions and the same number of cycles were used. In Figure 8, the reactivity profiles of the four natural Portuguese geological materials and wastes are represented together with the profile of SG1 and SG6, which are the one with best CaL performance.

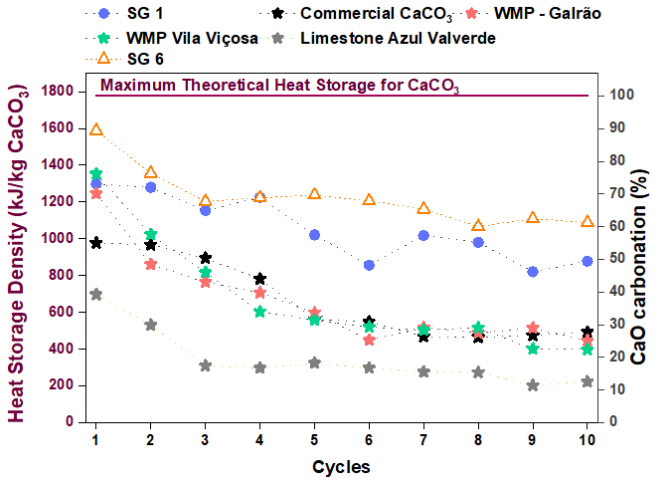

Figure 8 – Comparison of the heat storage density (kJ/kg $CaCO_3$) and CaO carbonation (%) of the SG1 (100 CaO) and SG6 (90CaO/10MgO) with a commercial $CaCO_3$, a natural limestone Azul Valverde, two waste marble powder (Galrão industry and Vila Viçosa quarry).

It is clear that the use of synthetic sorbents significantly improves reactivity during CaL. The natural sorbent with the best reactivity profile, in this case commercial $CaCO_3$, has an HSD of 492 kJ/kg $CaCO_3$, which is significantly lower than the HSDs of SG1 and SG6, which are 876 and 1088 kJ/kg $CaCO_3$, respectively. In the case of SG1, this represents a 78 % increase in HSD, while it is 121 % in SG6. On a theoretical level, it is clear that inert dopants and sol-gel synthesis significantly improve the efficiency of CaL for TCES, however, the feasibility of their implementation has to be considered from both an economic and technological perspective. With the use of these technologies, the production cost of the sorbents increases along with the difficulty to produce them on an industrial scale.

4. CONCLUSIONS

In many studies it is claimed that the use of steam improves the sorbent performance as it increases the S_{BET}. However, in this study, the use of steam had no long-term benefit on sorbent reactivity. The more steam is injected, the higher the S_{BET} after cycling, however this increase is due to the appearance of pores in the 3-10 nm range whose size is not beneficial for the CaL process. The CaO crystallite size increases with the steam increment, meaning that steam contributes to the sorbent sintering probably due to the higher thermal conductivity of steam relatively to air. Reducing the calcination temperature could be a solution to consider.

The performance of the Methocel™/CaO-based sorbent is lower than that of SG1 during all cycles, but its stability is higher due to its low deactivation. Furthermore, SG2 exhibits a low reduction in S_{BET} and a small increase in crystallite size, making it an excellent candidate for future research. In contrast to typical sintering and pore size change models, the sorbent's pore size has been observed to decrease towards the 20-30 nm range, so a better performance should be expected.

The SiC/CaO-based sorbents showed by far the worst results, with deactivation levels above 73% in all three samples. The S_{BET} loss is so large that it exceeds the LoQ (2 m^2/g) of the equipment, the mesopores observed in the fresh materials disappear after cycling and the increase in crystallite size is the largest of all samples (around 200%).

The best reactivity performance of the study was shown by SG6 (10% MgO) with an HSD of 1088 kJ/kg $CaCO_3$ at the 10th cycle, while SG7 and SG8 have a similar HSD to SG1. In general, the use of MgO as a dopant provides a better S_{BET} stability because the reduction after the cycles is lower than SG1.

CeO_2/CaO-based sorbents obtained similar results with a slightly lower HSD than SG1. In the first cycles, SG11 (30 % CeO_2) maintains a higher reactivity than the others until it gradually decays. The S_{BET} of the samples

have remained high compared to SG1, however the reduction of pore sizes between 10-100 nm, which are ideal for CaL, conditions the performance of the sorbent. Regarding the increase in crystallite size, all sorbents showed similar values. Due to its low performance and high production cost compared to MgO, the use of CeO_2 as a dopant in CaL under these operating conditions is questionable.

SG12 (10 MgO and 10CeO_2) was analysed with and without steam injection. The results indicate that the sample without steam injection has a better performance than SG1 and SG12 with steam.

From this study, it is evident that the use of dopant materials by sol-gel synthesis improves the reactivity during CaL compared to natural sorbents. Without using any dopant material, SG1 has increased the HSD of commercial $CaCO_3$ by 78%, while SG6 (supported with 10 MgO) has increased it by 121%.

5. REFERENCES

[1] I. E. A. IEA, "Electricity Market Report," *Electr. Mark. Rep.*, no. January, 2022, [Online]. Available: https://www.iea.org/reports/electricity-market-report-january-2022

[2] E. Union, "2030 Climate Target Plan." https://ec.europa.eu/clima/eu-action/european-green-deal/2030-climate-target-plan_en (accessed Aug. 03, 2022).

[3] X. Chen, Z. Zhang, C. Qi, X. Ling, and H. Peng, "State of the art on the high-temperature thermochemical energy storage systems," *Energy Convers. Manag.*, vol. 177, no. October, pp. 792–815, 2018, doi: 10.1016/j.enconman.2018.10.011.

[4] J. S. Prasad, P. Muthukumar, F. Desai, D. N. Basu, and M. M. Rahman, "A critical review of high-temperature reversible thermochemical energy storage systems," *Appl. Energy*, vol. 254, no. August, p. 113733, 2019, doi: 10.1016/j.apenergy.2019.113733.

[5] J. Blamey, E. J. Anthony, J. Wang, and P. S. Fennell, "The calcium looping cycle for large-scale CO 2 capture," *Prog. Energy Combust. Sci.*, vol. 36, no. 2, pp. 260–279, 2010, doi: 10.1016/j.pecs.2009.10.001.

[6] M. Benitez-Guerrero, J. M. Valverde, P. E. Sanchez-Jimenez, A. Perejon, and L. A. Perez-Maqueda, "Multicycle activity of natural CaCO3 minerals for thermochemical energy storage in Concentrated Solar Power plants," *Sol. Energy*, vol. 153, pp. 188–199, 2017, doi: 10.1016/j.solener.2017.05.068.

[7] J. Blamey, J. G. Yao, Y. Arai, and P. Fennell, *Enhancement of natural limestone sorbents for calcium looping processes*. Elsevier, 2015. doi: 10.1016/B978-0-85709-243-4.00005-7.

[8] P. Teixeira, E. Afonso, and C. I. C. Pinheiro, "Tailoring waste-derived materials for Calcium-Looping application in thermochemical energy storage systems," *J. CO2 Util.*, vol. 65, no. May, p. 102180, 2022, doi: 10.1016/j.jcou.2022.102180.

[9] E. T. Santos *et al.*, "Investigation of a stable synthetic sol – gel CaO sorbent for CO 2 capture," *Fuel*, vol. 94, pp. 624–628, 2012, doi: 10.1016/j.fuel.2011.10.011.

[10] V. Manovic and E. J. Anthony, "Thermal Activation of CaO-Based Sorbent and Self-Reactivation during CO 2 Capture Looping Cycles," vol. 42, no. 11, pp. 4170–4174, 2008.

[11] "Silicon Carbide, SiC Ceramic Properties," 2013. http://www.accuratus.com/silicar.html (accessed Sep. 18, 2022).

[12] J. Chen, L. Duan, and Z. Sun, "Review on the Development of Sorbents for Calcium Looping," *Energy and Fuels*, 2020, doi: 10.1021/acs.energyfuels.0c00682.

[13] "Engineering ToolBox," 2001. https://www.engineeringtoolbox.com/

[14] C. Luo, Q. Shen, N. Ding, Z. Feng, Y. Zheng, and C. Zheng, "Morphological Changes of Pure Micro- and Nano-Sized CaCO 3 during a Calcium Looping Cycle for CO 2 Capture," no. 3, pp. 547–554, 2012, doi: 10.1002/ceat.201000299.